Complex Modified Function Projective Lag Synchronization With Fixed-Time Stability Guarantees for Hyperchaotic Systems via a Fixed-Time Control Proposal

ANH TUAN VO [ID], THANH NGUYEN TRUONG, AND HEE-JUN KANG [ID]

Department of Electrical, Electronic and Computer Engineering, University of Ulsan, Ulsan 44610, South Korea

Corresponding author: Hee-Jun Kang (hjkang@ulsan.ac.kr)

ABSTRACT Our paper investigates complex modified function projective lag synchronization with fixed-time stability guarantees for hyperchaotic systems via a FxTC proposal. The synchronization of complex hyperchaotic systems and the desired performance are definitely guaranteed within a period of bounded time. The synchronization interval can be predefined without demanding the information of the initial conditions from the systems where the synchronization is performed. Furthermore, the fixed-time stability guarantees of the control scheme are achieved according to the Lyapunov principle and the settling time is calculated by solving the differential equations. In MATLAB/SIMULINK environment, synchronization performance from two simulation examples is performed in many cases with the change of initial values and time delay of the system to reveal the feasibility and the efficacy of the control proposal.

INDEX TERMS Fixed-time control theory, hyperchaotic complex systems, complex modified function projective lag synchronization.

I. INTRODUCTION

Synchronization of chaotic or hyperchaotic systems is a very important nonlinear behavior. This behavior is the consistent motion of two or more chaotic units originating with initial conditions discrepancy, it is formally defined in general, such as anti-synchronization, complete, phase or phase lag synchronization, and other forms of synchronization. This is a favorably appreciated research subject, initially formalized in theory and verified experimentally through the implementations of circuits [1]. Therefore, research on dynamic behavior and synchronization of the hyperchaotic systems with real variables has been popular in the scientific community. Their application potential is very large, the fields that have been successfully applied such as cryptography, biology, robotic, traffic forecasting, electrical engineering, quantum physics, and so on [2]–[5]. However, there exist several important scenarios of dynamic systems in which the state variables are complex values. Therefore, attention should be focused

The associate editor coordinating the review of this manuscript and approving it for publication was Ludovico Minati [ID].

on the study of chaotic and hyperchaotic nonlinear systems with complex variables. Some complex hyperchaotic systems have been introduced and analyzed their chaotic behaviors. For examples: In the study [6], the synchronization method has been applied for communication problem in which the time-delay was fully considered; In the paper [7], a complex set of Lorenz equations has been obtained from baroclinic instability and laser optics; A synchronization method has been introduced in paper [8] via passive synchronization of the HCSs for the improvement of secure communications. In addition, some other types of synchronizations of these systems have been studied including AS [9] or LS [10], [11]. All kinds of the mentioned synchronization can be considered for dynamical systems with real variables or complex variables. In addition, literature has also introduced several types of synchronization, including CoS [12], CoLS [13], PS [14], MPS [15], MPLS [16], and MFPS [17]. In recent years, various new synchronization types are only considered for chaotic complex nonlinear systems such as module-phase synchronization [18] and CPS [19]. In studies [18], [19], the behaviors of module and phase are fully considered. Besides,

in order to succeed in the synchronization of both module and phase, some different types of synchronization have been proposed by using complex scaling factors [20], [21]. This idea was first formed in research [22]. Then, it was extended and applied to many other studies, such as CCoS [23], CMPS [24], CFPS [25]. By using the scaling factors as functions or complex numbers, the unpredictability and complexity are extensively increased in those synchronization. Therefore, those factors significantly contribute to enhancing communication security [25]. From a practical point of view, the types of the presented synchronization are only rare scenarios of CMFPS. They are not general to all cases that can be found. Moreover, the time delay may occur between the master system and response system. In comparison with the types of the mentioned synchronization, the CMFPLS is a more general scenario [26], [27]. The type of this system is infrequently considered or not declared in recent studies. Therefore, our motivation is to handle CMFPLS problem of hyperchaotic systems via the new FxTC method in this paper.

In the literature, several control approaches such as Lyapunov-based active control methods [28], [29], passive control methods [30], [31], FnTC methods [32], [33], adaptive controllers [34] have been proposed so far to achieve suchlike complex synchronization of HCSs. Evaluating closely at the synchronization methods mentioned above, it is easy to see that synchronization methods such as [32], [33], or [34] have convergence time that depends on both the initial states and the control design parameters. The remaining synchronization methods can only guarantee an asymptotic convergence of synchronization errors. Therefore, achieving synchronization in a finite-time or fixed-time period is certainly a desirable goal for the next studies. As we know that FnTC approaches have been valuable and effective methods. The FnTC methods provide fast convergence in finite-time, robustness cope with uncertain terms or disturbances, and high tracking accuracy [35]. However, the drawback of the FnTC methods is related to the system's initial states. This can be an impediment to application to real systems when these initial states are unknown. To inherit the advantages of FnTC methods while overcoming their disadvantages, some scientists have introduced an improvement of finite-time stability theory. The main concept of the fixed-time stability theory is to design the control laws which can offer the desired convergence within a limited time [36]–[38]. That means the state trajectories of the system will be converged or stabilized to the origin in some finite time cases. Finite-time convergence is concerned with the controlled system's initial states, but fixed-time convergence is independent of those initial states. Therefore, the desired convergent time is completely established in advance through designed parameters.

Encouraged by the mentioned analysis, the core objective of this paper is to propose a new FxTC algorithm to achieve fixed-time CMFPLS of HCSs. Through the proposed control system, the CMFPLS errors converge to origin in an estimated period regardless of initial states, which means,

synchronization and stabilization will be achieved in the fixed-time period. The upper bound of the convergence time is estimated by assigning the design control parameters. The proof of synchronization and fixed-time stabilization has been fully verified through the Lyapunov theory. The important values of this paper can be summed up as follows:

- The CMFPLS of HCSs is considered. Applying this system, a new FxTC method is proposed to guarantee synchronization and the desired performance.
- Synchronization is not only achieved within a predefined limit of time regardless of initial values but the error states also are achieved finite-time convergence faster than some existing methods.
- The settling time is calculated by solving the differential equations and proof of stability and synchronization has been rigorously verified through Lyapunov theory.
- Two simulation examples are performed in many cases with the change of initial values and time delay of the system to verify the effectiveness of the designed method.

The organization of the paper is arranged as follows: some preliminaries, problem presentation, and motivations are presented in Section 2. Next, a new FxTC methodology is introduced to obtain the desired CMFPLS of HCSs. Section 4 presents two descriptive examples that are performed to validate the benefits of the proposed control method with detailed analysis. Finally, our paper ends with the remarkable conclusions in Section 5.

Annotations: The space of real number and complex number are symbolized $\mathbb{R}$ and $\mathbb{C}$, respectively. a block-diagonal matrix is indicated $diag(\cdot)$. For simplicity of expression, the following notation is defined as [35] $x^{[\phi]} = |x|^{\phi} sgn(x)$ with $x \in \mathbb{R}$ and $\phi > 0$. As $\phi \geqslant 1$ the derivative of the notation $x^{[\phi]}$ is described as $\frac{d}{dt}x^{[\phi]} = \phi|x|^{\phi-1}\dot{x}$. If $x \in \mathbb{C}$ i.e. in which $j = \sqrt{-1}$, superscripts r and c denote the real and imaginary elements of the state complex vector $\mathbf{x}$. $\mathbf{x} = [x_1, x_2, \ldots, x_n]^T \in \mathbb{R}^{\mathbf{n}}$ and $\mathbf{x} = [x_1, x_2, \ldots, x_n]^T \in \mathbb{C}^{\mathbf{n}}$ denote a state real vector and a state complex vector, respectively. T denotes transpose. $\bar{x} = x^r - jx^c$ denotes the complex conjugate of x. The following notation is adopted that $x^{[\phi]} = (x^r)^{[\phi]} + j(x^c)^{[\phi]}$.

Remark 1: Besides some of the synchronization types declared, the CMFPLS investigated in this analysis also included several other special cases including LAS, PLS, FPLS, MFPLS, CLAS, CFPLS, CMPLS, CLAS, CPLS, and CCoLS. Table 1 describes several types of synchronization.

II. PRELIMINARIES AND PROBLEM PRESENTATION
A. PRELIMINARIES
The following subsection states some theories belong to finite-time stability, fixed-time stability, and lemmas. Furthermore, synchronization and system description are also described, which is necessary for the next analysis.

The following system is given as

$$\dot{\mathbf{x}} = \Psi(t, \mathbf{x}), \quad \mathbf{x}(0) = \mathbf{x}_0 \qquad (1)$$

TABLE 1. Several categories of synchronization.

Types of synchronization		Function scaling matrix
$\tau = 0$	$\tau \neq 0$	$\xi(t) = \xi^r(t) + j\xi^c(t) = diag\,(\varpi_1(t), \varpi_2(t), \ldots, \varpi_n(t))$
		$\varpi_i(t) = \varpi_i^r(t) + j\varpi_i^c(t),\ (i = 1, \ldots, n)$
AS	LAS	$\varpi_i(t) = -1,\ (i = 1, \ldots, n)$
CoS	CoLS	$\varpi_i(t) = 1,\ (i = 1, \ldots, n)$
CAS	CLAS	$\varpi_i(t) = -1 - j,\ (i = 1, \ldots, n)$
CCoS	CCoLS	$\varpi_i(t) = 1 + j,\ (i = 1, \ldots, n)$
PS	PLS	$\varpi_i^r(t),\ (i = 1, \ldots, n)$ represent identical real constants and $\xi^c(t) = 0$
MPS	MPLS	$\varpi_i^r(t),\ (i = 1, \ldots, n)$ represent identical real constants and $\xi^c(t) = 0$
FPS	FPLS	$\varpi_i^r(t),\ (i = 1, \ldots, n)$ represent identical real functions and $\xi^c(t) = 0$
MFPS	MFPLS	$\varpi_i^r(t),\ (i = 1, \ldots, n)$ represent identical real functions and $\xi^c(t) = 0$
CPS	CPLS	$\varpi_i(t),\ (i = 1, \ldots, n)$ represent identical complex constants and $\xi^c(t) = 0$
CMPS	CMPLS	$\varpi_i(t),\ (i = 1, \ldots, n)$ represent different complex constants and $\xi^c(t) = 0$
CFPS	CFPLS	$\varpi_i(t),\ (i = 1, \ldots, n)$ represent identical complex functions and $\xi^c(t) = 0$

whereas $\mathbf{x} \in \mathbb{R}^n$ and $\Psi: \mathbb{R}_+ \times \mathbb{R}^n \to \mathbb{R}^n$ is a nonlinear function, it can be discontinuous. Suppose that the origin is an equilibrium point of the system (1).

Remark 2: The differential equation (1) is the expression of most of the familiar chaotic (hyperchaotic) complex systems. They can be listed as Lü systems, Lorenz, and chaotic (hyperchaotic) complex Chen, etc.

Definition 1 [39]: The equilibrium point of Eq. (1) is considered to be globally finite-time stable in case it is globally asymptotically stable and any solution $\mathbf{x}(t, \mathbf{x}_0)$ of Eq. (1) converge to the equilibria within the finite-time period, i.e. $\mathbf{x}(t, \mathbf{x}_0) = 0, \forall t \geqslant T(\mathbf{x}_0)$, where $T : \mathbb{R}^n \to \mathbb{R}_+ \cup \{0\}$ is the settling–time function.

Definition 2 [39]: The equilibrium point of Eq. (1) is considered to be a fixed-time stable equilibrium point in case it also is globally finite-time stable within bounded settling-time function $T(\mathbf{x}_0)$, i.e. $\exists T_{\max} > 0 : T(\mathbf{x}_0) \leqslant T_{\max}, \ \forall \mathbf{x}_0 \in \mathbb{R}^n$.

Lemma 1 [40]: For any real numbers $\rho_1, \rho_2 > 0$ and $0 < \beta < 1$, an extended Lyapunov function condition of finite-time stability is presented in the form as $\dot{L}(x) + \rho_1 L(x) + \rho_2 L^\beta(x) \leqslant 0$, where convergence time is calculated and bounded by the following inequality:

$$T \leqslant \frac{1}{\rho_1(1 - \beta)} \ln \frac{\rho_1 V(x(0))^{1-\beta} + \rho_2}{\rho_2} \qquad (2)$$

Lemma 2 [41]: That is termed Jensen's inequality:

$$\left(\sum_{i=1}^m z_i^{\theta_2}\right)^{1/\theta_2} \leqslant \left(\sum_{i=1}^m z_i^{\theta_1}\right)^{1/\theta_1}, \quad 0 < \theta_1 < \theta_2 \qquad (3)$$

where $z_i \geqslant 0$ and $0 \leqslant i \leqslant m$.

B. PROBLEM PRESENTATION

In this study, two different n-dimensional HCSs are described as follows. Master system and slave system are described by the following expressions, respectively.

$$\dot{\mathbf{x}}(t) = \mathbf{f}\,(\mathbf{x}(t), \bar{\mathbf{x}}(t), t) \qquad (4)$$
$$\dot{\mathbf{y}}(t) = \mathbf{h}\,(\mathbf{y}(t), \bar{\mathbf{y}}(t), t) + \mathbf{u}(t) \qquad (5)$$

where $\mathbf{x}(t)$ and $\mathbf{y}(t)$ are the state complex vector. $\dot{\mathbf{x}}(t) = \dot{\mathbf{x}}^r(t) + j\dot{\mathbf{x}}^c(t)$ and $\dot{\mathbf{y}}(t) = \dot{\mathbf{y}}^r(t) + j\dot{\mathbf{y}}^c(t)$. $\mathbf{f}\,(\mathbf{x}(t), \bar{\mathbf{x}}(t), t)$ and $\mathbf{h}\,(\mathbf{y}(t), \bar{\mathbf{y}}(t), t)$ are the vector of nonlinear complex functions of the master system and the response system, respectively. $\mathbf{u}(t)$ is the vector of control inputs.

The CMFPLS errors between the master system and the slave system is defined by the following equation:

$$\mathbf{e}(t) = \mathbf{y}(t) - \xi(t)\mathbf{x}(t - \tau) \qquad (6)$$

where $\xi(t) = \xi^r(t) + j\xi^c(t)$, $\xi(t) = diag\,(\varpi_1(t), \varpi_2(t), \ldots, \varpi_n(t))$ stands for scaling function matrix. All factors $\varpi_i(t) = \varpi_i^r(t) + j\varpi_i^c(t) \in \mathbb{C}, (i = 1, \ldots, n)$ should be continuously differentiable bounded function and $\varpi_i(t) \neq 0$ for all $t > 0$. τ is positive time lag, $\mathbf{e}(t) = \mathbf{e}^r(t) + j\mathbf{e}^c(t)$, $\mathbf{e}(t) = [e_1(t), e_2(t), \ldots, e_n(t)]^T$, $\mathbf{e}^r = \left[e_1^r, e_2^r, \ldots, e_n^r\right]^T$, and $\mathbf{e}^c = \left[e_1^c, e_2^c, \ldots, e_n^c,\right]^T$.

Taking time derivative of Eq. (6), one has:

$$\begin{aligned}
\dot{\mathbf{e}}(t) &= \dot{\mathbf{y}}(t) - \dot{\xi}(t)\mathbf{x}(t - \tau) - \xi(t)\dot{\mathbf{x}}(t - \tau) \\
&= \mathbf{h}\,(\mathbf{y}(t), \bar{\mathbf{y}}(t), t) + \mathbf{u}(t) - \dot{\xi}(t)\mathbf{x}(t - \tau) \\
&\quad - \xi(t)\mathbf{f}\,(\mathbf{x}(t - \tau), \bar{\mathbf{x}}(t - \tau), t - \tau) \qquad (7)
\end{aligned}$$

A set of the following differential equations is rewritten from Eq. (7):

$$\begin{aligned}
\dot{e}_i(t) &= h_i\,(\mathbf{y}(t), \bar{\mathbf{y}}(t), t) + u_i(t) - \dot{\varpi}_i(t)\mathbf{x}(t - \tau) \\
&\quad - \varpi_i(t)f_i\,(\mathbf{x}(t - \tau), \bar{\mathbf{x}}(t - \tau), t - \tau) \qquad (8)
\end{aligned}$$

Definition 3 [42]: The CMFPLS errors between the master system (4) and the slave system (5) will be converged to zero within a period of fixed-time if there exists a time moment $T > 0$, which does not depend on the system' initial error states, $\mathbf{e}\,(t_0)$, such that $\|\mathbf{e}\,(t)\| = 0, \forall t \geqslant t_0 + T$.

The central motivation of the paper can be summed up as follows.

This article proposes the new control laws $u_i(t), (i = 1, \ldots, n)$ to achieve fixed-time CMFPLS of HCSs. Through the proposed control laws, the CMFPLS errors converge to origin in an estimated period of time regardless of initial states, i.e., synchronization and stabilization will be achieved in the fixed-time period according to the meaning of Definition 3.

III. CONTROL DESIGN APPROACH

To attain the main control objective with the desired performance, a suitable feedback control algorithm is designed based on Eq. (8) and the FxTC theory as follows.

$$
\begin{aligned}
u_i(t) &= u_i^r(t) + j u_i^c(t) \\
&= -h_i\left(\mathbf{y}(t), \bar{\mathbf{y}}(t), t\right) + \dot{\varpi}_i(t)\mathbf{x}(t-\tau) \\
&\quad + \varpi_i(t) f_i\left(\mathbf{x}(t-\tau), \bar{\mathbf{x}}(t-\tau), t-\tau\right) \\
&\quad - \kappa_{1i} e_i^{[2-\alpha_i]} - \kappa_{2i}\left([\bar{e}]^{\lambda_i|e_i^r|} e_i^r + j[\bar{e}]^{\lambda_i|e_i^c|} e_i^c\right) \\
&\quad - \kappa_{3i} e_i^{[\alpha_i]} - \Gamma_i e_i
\end{aligned}
\tag{9}
$$

where $\lambda_i, \Gamma_i > 0$, $0 < \alpha_i < 1$, $\kappa_{1i}, \kappa_{2i}, \kappa_{3i}$ are positive constants that are designed to be bounded condition $4\kappa_{1i}\kappa_{3i} > \kappa_{2i}^2$, $(i = 1, \ldots, n)$ and $[\bar{e}]$ stands for the Euler's number.

The following theorem is synthesized for control design and proof of fixed-time stability.

Theorem 1: If the CMFPLS errors between the master system (4) and the slave system (5) are controlled by the proposed control system in Eq. (9), then the error dynamics given by Eqs. (6) – (8) are forced to move from initial values to the origin with a globally fixed-time stable, T, determined by the following equation:

$$
\begin{aligned}
T = {} & \frac{1}{(1-\alpha_i)} \frac{2}{\sqrt{4\kappa_{1i}\kappa_{3i} - \kappa_{2i}^2}} \\
& \times \left(\frac{\pi}{2} - \arctan\frac{\kappa_{2i}}{\sqrt{4\kappa_{1i}\kappa_{3i} - \kappa_{2i}^2}}\right)
\end{aligned}
\tag{10}
$$

Proof of Theorem 1 is verified in the two following steps.

Step 1: We prove that under the drive of the control laws (9), system (8) will achieve asymptotic stability, which means that the equilibrium of Eq. (8) is indeed a is globally asymptotically stable based on the Lyapunov theory as the meaning in Definition 2.

Proof: Applying the proposed controller designed in Eq. (9) to error dynamics (8), one has:

$$
\begin{aligned}
\dot{e}_i &= \dot{e}_i^r + j\dot{e}_i^c \\
&= -\kappa_{1i} e_i^{[2-\alpha_i]} - \kappa_{2i}\left([\bar{e}]^{\lambda_i|e_i^r|} e_i^r + j[\bar{e}]^{\lambda_i|e_i^c|} e_i^c\right) \\
&\quad - \kappa_{3i} e_i^{[\alpha_i]} - \Gamma_i e_i
\end{aligned}
\tag{11}
$$

Remark 3: The role of each part in Eq. (9) or differential equation (11) is expressed as follows. When $|e_i| > 1$, $\left|-\kappa_{1i} e_i^{[2-\alpha_i]} - \kappa_{2i}\left([\bar{e}]^{\lambda_i|e_i^r|} e_i^r + j[\bar{e}]^{\lambda_i|e_i^c|} e_i^c\right) - \Gamma_i e_i\right|$ plays the principal function that provides a fast convergence rate from any initial condition to 1. When $|e_i|$ is much smaller than 1, $\left|-\kappa_{3i} e_i^{[\alpha_i]}\right|$ expresses the main function that offers finite-time convergence. Once synchronization errors $\left|e_i^r\right|$ or $\left|e_i^c\right|$ converge to the neighborhood of zero then the gains $\kappa_{2i}[\bar{e}]^{\lambda_i|e_i^r|}$ and $\kappa_{2i}[\bar{e}]^{\lambda_i|e_i^c|}$ will be reduced to a small value. It infers that the role of $\left|-\kappa_{3i} e_i^{[\alpha_i]}\right|$ is very robust in the phase of the finite-time convergence.

Then, the result in Eq. (11) can be rearranged with the following expression:

$$
\begin{cases}
\dot{e}_i^r = -\kappa_{1i}\left(e_i^r\right)^{[2-\alpha_i]} - \kappa_{2i}[\bar{e}]^{\lambda_i|e_i^r|} e_i^r \\
\qquad - \kappa_{3i}\left(e_i^r\right)^{[\alpha_i]} - \Gamma_i e_i^r \\
\dot{e}_i^c = -\kappa_{1i}\left(e_i^c\right)^{[2-\alpha_i]} - \kappa_{2i}[\bar{e}]^{\lambda_i|e_i^c|} e_i^c \\
\qquad - \kappa_{3i}\left(e_i^c\right)^{[\alpha_i]} - \Gamma_i e_i^c
\end{cases}
\tag{12}
$$

Selecting a positive definite function as a Lyapunov function candidate as:

$$
L = \sum_{i=1}^{n}\left(e_i^r\right)^2 + \sum_{i=1}^{n}\left(e_i^c\right)^2
\tag{13}
$$

Calculating time derivative of Lyapunov function candidate in Eq. (13) yields:

$$
\dot{L} = 2\sum_{i=1}^{n} e_i^r \dot{e}_i^r + 2\sum_{i=1}^{n} e_i^c \dot{e}_i^c
\tag{14}
$$

Substituting the trajectories in Eq. (12) into Eq. (14) gives:

$$
\begin{aligned}
\dot{L} = {} & 2\sum_{i=1}^{n} e_i^r \left(\begin{array}{l} -\kappa_{1i}\left(e_i^r\right)^{[2-\alpha_i]} - \kappa_{2i}[\bar{e}]^{\lambda_i|e_i^r|} e_i^r \\ -\kappa_{3i}\left(e_i^r\right)^{[\alpha_i]} - \Gamma_i e_i^r \end{array}\right) \\
& + 2\sum_{i=1}^{n} e_i^c \left(\begin{array}{l} -\kappa_{1i}\left(e_i^c\right)^{[2-\alpha_i]} - \kappa_{2i}[\bar{e}]^{\lambda_i|e_i^c|} e_i^c \\ -\kappa_{3i}\left(e_i^c\right)^{[\alpha_i]} - \Gamma_i e_i^c \end{array}\right) \\
= {} & 2\sum_{i=1}^{n} \left(\begin{array}{l} -\kappa_{1i}\left(e_i^r\right)^{[3-\alpha_i]} - \kappa_{2i}[\bar{e}]^{\lambda_i|e_i^r|}\left(e_i^r\right)^2 \\ -\kappa_{3i}\left(e_i^r\right)^{[\alpha_i+1]} - \Gamma_i\left(e_i^r\right)^2 \end{array}\right) \\
& + 2\sum_{i=1}^{n} \left(\begin{array}{l} -\kappa_{1i}\left(e_i^c\right)^{[3-\alpha_i]} - \kappa_{2i}[\bar{e}]^{\lambda_i|e_i^c|}\left(e_i^c\right)^2 \\ -\kappa_{3i}\left(e_i^c\right)^{[\alpha_i+1]} - \Gamma_i\left(e_i^c\right)^2 \end{array}\right)
\end{aligned}
\tag{15}
$$

From Eq. (15), it is seen that $[\bar{e}]^{\lambda_i|e_i^r|}\left(e_i^r\right)^2 \geq \left(e_i^r\right)^2$, $[\bar{e}]^{\lambda_i|e_i^c|}\left(e_i^c\right)^2 \geq \left(e_i^c\right)^2$, and $(-\kappa_{2i} - \Gamma_i < -\kappa_{2i})$. Therefore,

$$
\begin{aligned}
\dot{L} \leq {} & 2\sum_{i=1}^{n}\left(-\kappa_{1i}\left[\left(e_i^r\right)^{[3-\alpha_i]} + \left(e_i^c\right)^{[3-\alpha_i]}\right]\right) \\
& + 2\sum_{i=1}^{n}\left(-\kappa_{2i}\left[\left(e_i^r\right)^2 + \left(e_i^c\right)^2\right]\right) \\
& + 2\sum_{i=1}^{n}\left(-\kappa_{3i}\left[\left(e_i^r\right)^{[\alpha_i+1]} + \left(e_i^c\right)^{[\alpha_i+1]}\right]\right)
\end{aligned}
\tag{16}
$$

Applying Jensen's inequality stated in Lemma 2, one has:

$$
\begin{aligned}
\dot{L} \leq {} & 2\sum_{i=1}^{n}\left(-\kappa_{1i}\left[\left(e_i^r\right)^2 + \left(e_i^c\right)^2\right]^{\frac{3-\alpha_i}{2}}\right) \\
& + 2\sum_{i=1}^{n}\left(-\kappa_{2i}\left[\left(e_i^r\right)^2 + \left(e_i^c\right)^2\right]\right) \\
& + 2\sum_{i=1}^{n}\left(-\kappa_{3i}\left[\left(e_i^r\right)^2 + \left(e_i^c\right)^2\right]^{\frac{\alpha_i+1}{2}}\right) \\
\leq {} & -2\kappa_{1i} L^{\frac{3-\alpha_i}{2}} - 2\kappa_{2i} L - 2\kappa_{3i} L^{\frac{\alpha_i+1}{2}}
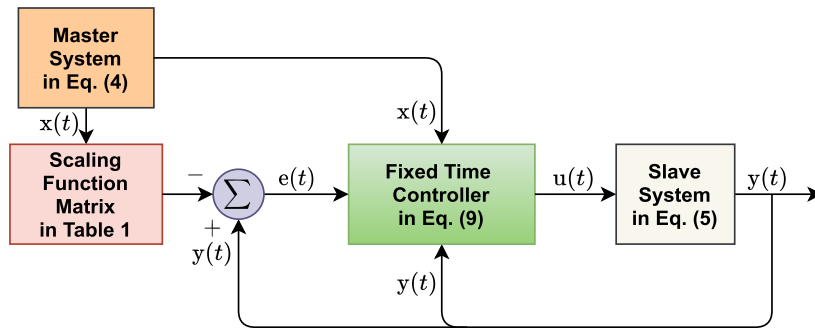\end{aligned}
\tag{17}
$$

FIGURE 1. Block diagram of the proposed control system.

According to Eq. (17), it is clear that $\dot{L} \leq 0$ and $L > 0$. Therefore, we can conclude that origin of Eq. (8) or Eq. (12) is globally asymptotically stable under the proposed controller (9) based on the Lyapunov theory.

Step 2: We keep indicating that the convergence can be obtained in finite-time.

Based on Eq. (17), the following differential equation is considered.

$$\dot{\vartheta} = -2\kappa_{1i}\vartheta^{\frac{3-\alpha_i}{2}} - 2\kappa_{2i}\vartheta - 2\kappa_{3i}\vartheta^{\frac{\alpha_i+1}{2}}, \quad \vartheta(0) = \vartheta_0 \geq 0$$
$$= -2\left(\kappa_{1i}\vartheta^{1-\alpha_i} + \kappa_{2i}\vartheta^{\frac{1-\alpha_i}{2}} + \kappa_{3i}\right)\vartheta^{\frac{\alpha_i+1}{2}} \quad (18)$$

Eq. (18) is corresponding to the following expression:

$$dt = -\frac{d\vartheta}{2\left(\kappa_{1i}\vartheta^{1-\alpha_i} + \kappa_{2i}\vartheta^{\frac{1-\alpha_i}{2}} + \kappa_{3i}\right)\vartheta^{\frac{\alpha_i+1}{2}}} \quad (19)$$

We have $d\vartheta^{\frac{1-\alpha_i}{2}} = \frac{1-\alpha_i}{2}\vartheta^{-\frac{\alpha_i+1}{2}}d\vartheta \Rightarrow d\vartheta = \frac{2d\vartheta^{\frac{1-\alpha_i}{2}}}{1-\alpha_i}\vartheta^{\frac{\alpha_i+1}{2}}$. Hence, Eq. (19) is rewritten as:

$$dt = -\frac{1}{1-\alpha_i}\frac{d\vartheta^{\frac{1-\alpha_i}{2}}}{\left(\kappa_{1i}\vartheta^{1-\alpha_i} + \kappa_{2i}\vartheta^{\frac{1-\alpha_i}{2}} + \kappa_{3i}\right)} \quad (20)$$

Taking the integral of both sides of Eq. (20), we have:

$$\int_0^{t_{e_i}} dt = \frac{1}{1-\alpha_i}\int_0^{\vartheta(0)}\frac{d\vartheta^{\frac{1-\alpha_i}{2}}}{\left(\kappa_{1i}\vartheta^{1-\alpha_i} + \kappa_{2i}\vartheta^{\frac{1-\alpha_i}{2}} + \kappa_{3i}\right)}$$
$$= \frac{1}{(1-\alpha_i)}\frac{2}{\sqrt{4\kappa_{1i}\kappa_{3i} - \kappa_{2i}^2}}\left(\begin{array}{c}\arctan\frac{2\kappa_{1i}\vartheta^{\frac{1-\alpha_i}{2}}(0)+\kappa_{2i}}{\sqrt{4\kappa_{1i}\kappa_{3i}-\kappa_{2i}^2}} \\ -\arctan\frac{\kappa_{2i}}{\sqrt{4\kappa_{1i}\kappa_{3i}-\kappa_{2i}^2}}\end{array}\right) \quad (21)$$

The calculated result in Eq. (21) is explained in Appendix in detail.

Eq. (21) shows that $\vartheta(0)$ will converge to zero in finite time T_ϑ as follows:

$$T_\vartheta$$
$$= \frac{1}{(1-\alpha_i)}\frac{2}{\sqrt{4\kappa_{1i}\kappa_{3i} - \kappa_{2i}^2}}$$

$$\times\left(\arctan\frac{2\kappa_{1i}\vartheta^{\frac{1-\alpha_i}{2}}(0)+\kappa_{2i}}{\sqrt{4\kappa_{1i}\kappa_{3i}-\kappa_{2i}^2}} - \arctan\frac{\kappa_{2i}}{\sqrt{4\kappa_{1i}\kappa_{3i}-\kappa_{2i}^2}}\right) \quad (22)$$

According to the comparison principle [43], we can obtain that $L(t) \leq \vartheta(t)$ when $L(t=0) \leq \vartheta_0$, it follow that $L(t)$, and therefore the origin of (9), reach zero within a period of finite-time $T_L \leq T_\vartheta$, with

$$T_L$$
$$= \frac{1}{(1-\alpha_i)}\frac{2}{\sqrt{4\kappa_{1i}\kappa_{3i} - \kappa_{2i}^2}}$$

$$\times\left(\arctan\frac{2\kappa_{1i}L^{\frac{1-\alpha_i}{2}}(0)+\kappa_{2i}}{\sqrt{4\kappa_{1i}\kappa_{3i}-\kappa_{2i}^2}} - \arctan\frac{\kappa_{2i}}{\sqrt{4\kappa_{1i}\kappa_{3i}-\kappa_{2i}^2}}\right) \quad (23)$$

Based on definition 1 and the result in Eq. (23), we can conclude that the equilibrium point of Eq. (12) is globally finite-time stable.

It can be easy to show that T_L is bounded by:

$$T_L \leq T = \frac{1}{(1-\alpha_i)}\frac{2}{\sqrt{4\kappa_{1i}\kappa_{3i} - \kappa_{2i}^2}}$$
$$\times\left(\frac{\pi}{2} - \arctan\frac{\kappa_{2i}}{\sqrt{4\kappa_{1i}\kappa_{3i}-\kappa_{2i}^2}}\right) \quad (24)$$

The convergence time T is only reliant on the design parameters as shown in Eq. (24). Therefore, the origin of error dynamics (12) is concluded by definition 3 as globally fixed-time stable. In other words, through the proposed control laws (9), synchronization and stabilization have been achieved in the fixed-time period according to the meaning of Definition 3. The evidence of theorem 1 has been fully confirmed.

Block diagram of the proposed control system is summarily described in Fig. 1.

Remark 4: The proposed control algorithm stated in this paper could be applied to every one of the chaos control systems or types of synchronization between hyperchaotic

systems which have non-square scaling factor matrices and different orders.

Remark 5: The advantage of our method in comparison with some existing methods [44]–[49] for synchronization problems is to guarantee that as long as the control design parameters are accounted for, synchronization can be achieved within a finite time. In other words, the convergence (settling) time is calculated based on the unique design constants without any dependence on the initial state of the systems. This article provides an algorithm that a priori guarantees any desired value of the convergence time for the synchronization. Based on a careful review of the mentioned works, we discover that the works [46], [48] achieve synchronization within a finite-time; however, the convergence time is affected by both the designed control parameters and the initial conditions of the systems; the works [44], [45], [47], [49] only guarantee to obtain asymptotic synchronization ($\lim_{t \to +\infty} |e_i| = 0$). Recent developments have emphasized the importance of finite-time synchronization and it is more expected.

The proposed method provides robust stabilization performance. However, we have not considered the effects of the changing (time-varying) uncertainties and external disturbances in this paper. We know that the strong ability of SMC algorithms is against time-varying uncertainties and external disturbances, our next work is to research the CMFPLS of HCSs with the mentioned uncertain terms by proposing a new fixed-time SMC.

IV. NUMERICAL SIMULATION
In this section, two descriptive examples are performed in MATLAB/SIMULINK environment to validate the benefits of the proposed control method with detailed analysis. To solve differential equations, the fourth-order Runge-Kutta method is employed with a time step size of 10^{-3}s in all the simulations.

A. THE FIRST ILLUSTRATIVE EXAMPLE
The first illustrative example presents the CMPS between two hyperchaotic systems under the pressure of the proposed controller. The CMPS performance from the proposed method is compared to the existing algorithm [50] to evaluate its effectiveness. For a reasonable evaluation, the compared chaotic complex systems and their control parameters were directly taken in the study [50].

We assumed that the chaotic complex Lorenz system is used as the master system with the following equation:

$$\dot{\mathbf{x}}(t) = \mathbf{f}(\mathbf{x}(t), \bar{\mathbf{x}}(t), t) \qquad (25)$$

where $\dot{\mathbf{x}}(t) = \begin{bmatrix} x_1, & x_2, & x_3 \end{bmatrix}^T$
and $\mathbf{f}(\mathbf{x}(t), \bar{\mathbf{x}}(t), t) = \begin{bmatrix} 14(x_2 - x_1) \\ 35x_1 - x_2 - x_1 x_3 \\ 1/2(\bar{x}_1 x_2 + x_1 \bar{x}_2) - 3.7x_3 \end{bmatrix}$.

The slave system is selected as the chaotic complex Lu system described in the below equations:

$$\dot{\mathbf{y}}(t) = \mathbf{h}(\mathbf{y}(t), \bar{\mathbf{y}}(t), t) + \mathbf{u}(t) \qquad (26)$$

in which $\dot{\mathbf{y}}(t) = \begin{bmatrix} y_1, & y_2, & y_3 \end{bmatrix}^T$,
$\mathbf{h}(\mathbf{y}(t), \bar{\mathbf{y}}(t), t) = \begin{bmatrix} 40(y_2 - y_1) \\ 22y_2 - y_1 y_3 \\ 1/2(\bar{y}_1 y_2 + y_1 \bar{y}_2) - 5y_3 \end{bmatrix}$,
and $\mathbf{u}(t) = \begin{bmatrix} u_1, & u_2, & u_3 \end{bmatrix}^T$.

The master system (25) and the slave system (26) have the initial conditions $\mathbf{x}(0)$ and $\mathbf{y}(0)$ selected accordingly as in Table 2. To obtain the CMPS, the time delay τ and the factor scaling function ξ are respectively selected according to Table 1 and they are stated in Table 2. The proposed controller parameters are assigned as in Table 2 for the first illustrative example. From the controller parameters in Table 2, we can calculate the upper bound of convergence time with $T_1 \approx 2.0154(s)$, which is based on Eq. (24). This upper bound value only depends on design constants and does not depend on the initial states of the synchronized system. To reinforce this point, the first illustrative example is performed in two cases. The initial conditions of both systems set up for the two cases are presented in Table 2.

For the first illustrative example, the root-mean-square errors are calculated in 12 seconds, as reported in Table 3. The convergence time of the CMPS error states under the two different control methods are shown in Table 4.

For both cases, the synchronization performances including the CMPS errors and the state trajectories under varying time from the master system and the slave system are illustrated in Fig. 2 and Fig. 3, respectively. As described in Figs. 2, 3 and Table 4, the time convergence of the CMPS errors can be obtained within a period of limited time that is lesser than $T_1 \approx 2.0154(s)$. While the CMPS errors under the method in [50] only obtain an asymptotic convergence and stabilization, as shown in the enlarged images of the CMPS errors, i.e., $\lim_{t \to +\infty} |e_i| = 0$. From the performance exhibited in Fig. 2 and Fig. 3, it is easy to see that the fixed-time CMPS has been completely achieved between the two presented systems. The proposed control system not only provides fixed-time synchronization but also achieves synchronization much faster than the compared method, as reported in Table 4. Therefore, it can be concluded that the proposed control law provides better synchronous performance than the synchronous performance from the study [50].

B. THE SECOND ILLUSTRATIVE EXAMPLE
The second illustrative example describes the achievement of CMFPLS in the fixed-time period from two HCSs to validate the proposed theoretical result further and fully. The hyperchaotic complex Lu system is applied as the master system and the hyperchaotic complex Lorenz system is performed as the response system.

TABLE 2. Control parameters and system parameters.

$(i = 1, 2, 3)$	Symbol	Value
Control parameter	$\kappa_{1i}, \kappa_{2i}, \kappa_{3i}, \lambda_i, \alpha_i, \Gamma_i$	$3, 3, 3, 0.1, 0.8, 3$
	ξ	$diag(1, -1, 0)$
	τ	0
Initial condition in **case 1**	$\mathbf{x}(0)$	$\begin{bmatrix} -3 + j2, & -3 + j4, & 6 \end{bmatrix}^T$
	$\mathbf{y}(0)$	$\begin{bmatrix} 5 + j4, & -4 + j2, & 3 \end{bmatrix}^T$
Initial condition in **case 2**	$\mathbf{x}(0)$	$10 * \begin{bmatrix} -3 + j2, & -3 + j4, & 6 \end{bmatrix}^T$
	$\mathbf{y}(0)$	$\begin{bmatrix} 5 + j4, & -4 + j2, & 3 \end{bmatrix}^T$

TABLE 3. RMSE under the two different control methods.

Control Method	RMSE($e_1^r(t)$)	RMSE($e_1^c(t)$)	RMSE($e_2^r(t)$)	RMSE($e_2^c(t)$)
Case 1: $\mathbf{x}(0) = \begin{bmatrix} -3 + j2, & -3 + j4, & 6 \end{bmatrix}^T$ and $\mathbf{y}(0) = \begin{bmatrix} 5 + j4, & -4 + j2, & 3 \end{bmatrix}^T$				
Control method [50]	0.9442	0.2360	0.8262	0.7081
Proposed method	0.4326	0.1164	0.3836	0.3330
Case 2: $\mathbf{x}(0) = 10 * \begin{bmatrix} -3 + j2, & -3 + j4, & 6 \end{bmatrix}^T$ and $\mathbf{y}(0) = \begin{bmatrix} 5 + j4, & -4 + j2, & 3 \end{bmatrix}^T$				
Control method [50]	4.1308	1.8884	4.0128	4.9570
Proposed method	1.2010	0.7695	1.1882	1.2714

TABLE 4. Control parameters and system parameters.

$(i = 1, 2, 3, 4)$	Symbol	Value
Control parameter	$\kappa_{1i}, \kappa_{2i}, \kappa_{3i}, \lambda_i, \alpha_i, \Gamma_i$	$2, 1, 2, 0.1, 0.65, 3$
Initial condition	$\mathbf{x}(0)$	$\begin{bmatrix} 2 + j6, & 7 - j5, & 5, & -1 \end{bmatrix}^T$
	$\mathbf{y}(0)$	$\sigma * \begin{bmatrix} -1 + j2, & -2 + j3, & 4, & -3 \end{bmatrix}^T$
	σ	$\{-3, -2, 1.5, 2, 4, 3\}$
	ξ	$diag(1 + j\sin(t), 2 - j\cos(t), 1.5, \cos(2t))$
	τ_1, τ_2	$0.1, 0.3$

TABLE 5. RMSE under the proposed control method.

	$\sigma = -3$	$\sigma = -2$	$\sigma = 1.5$	$\sigma = 2$	$\sigma = 4$	$\sigma = 3$
In Case: $\tau_1 = 0.1$, $t_0 = 3s$, and $\sigma = \{-3, -2, 1.5, 2, 4, 3\}$						
RMSE($e_1^r(t)$)	1.6723	1.6697	1.9640	1.5803	1.3369	1.3907
RMSE($e_1^c(t)$)	1.1000	1.3220	0.4684	0.3206	0.4415	0.4110
RMSE($e_2^r(t)$)	2.1702	2.1642	2.4672	2.1314	2.0327	2.0295
RMSE($e_2^c(t)$)	0.0263	0.0848	0.1190	1.4298	0.6380	0.5968
RMSE($e_3(t)$)	1.3933	1.0187	2.3350	2.2854	1.9775	2.0697
RMSE($e_4(t)$)	0.7991	1.2012	1.0568	0.9364	0.1815	0.3928
In Case: $\tau_2 = 0.3$, $t_0 = 3s$, and $\sigma = \{-3, -2, 1.5, 2, 4, 3\}$						
RMSE($e_1^r(t)$)	0.7674	0.7635	1.2263	0.6316	0.2842	0.3599
RMSE($e_1^c(t)$)	1.0211	1.2499	0.3730	0.4174	0.3454	0.3140
RMSE($e_2^r(t)$)	1.3457	1.3329	2.0601	1.2644	1.0674	1.0612
RMSE($e_2^c(t)$)	0.3835	0.4864	0.2972	1.1376	0.2538	0.2080
RMSE($e_3(t)$)	0.8433	1.2421	1.1414	0.9814	0.1605	0.3835
RMSE($e_4(t)$)	1.8669	2.0842	0.4261	0.5656	1.2460	1.0841

Description of the master system is given as the following equations:

$$\dot{\mathbf{x}}(t) = \mathbf{f}(\mathbf{x}(t), \bar{\mathbf{x}}(t), t) \tag{27}$$

whereas

$$\dot{\mathbf{x}}(t) = \begin{bmatrix} x_1, & x_2, & x_3, & x_4 \end{bmatrix}^T,$$

$$\mathbf{f}(\mathbf{x}(t), \bar{\mathbf{x}}(t), t) = \begin{bmatrix} 42(x_2 - x_1) + x_4 \\ 25x_2 - x_1 x_3 + x_4 \\ 1/2(\bar{x}_1 x_2 + x_1 \bar{x}_2) - 6x_3 \\ 1/2(\bar{x}_1 x_2 + x_1 \bar{x}_2) - 5x_4 \end{bmatrix},$$
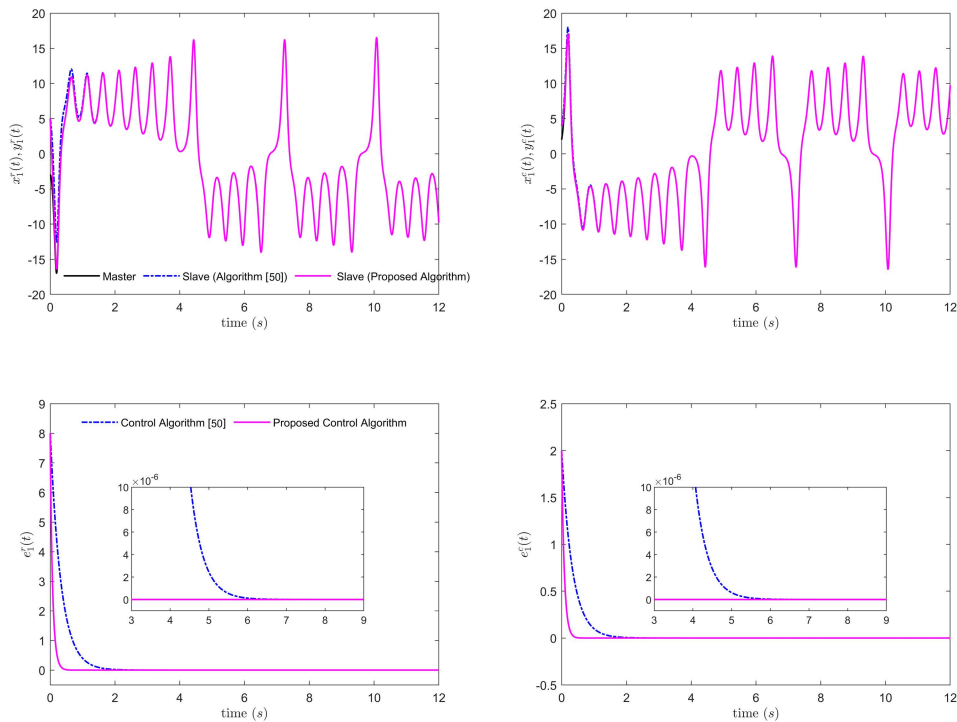
and description of the slave system is given by:

$$\dot{\mathbf{y}}(t) = \mathbf{h}(\mathbf{y}(t), \bar{\mathbf{y}}(t), t) + \mathbf{u}(t) \tag{28}$$
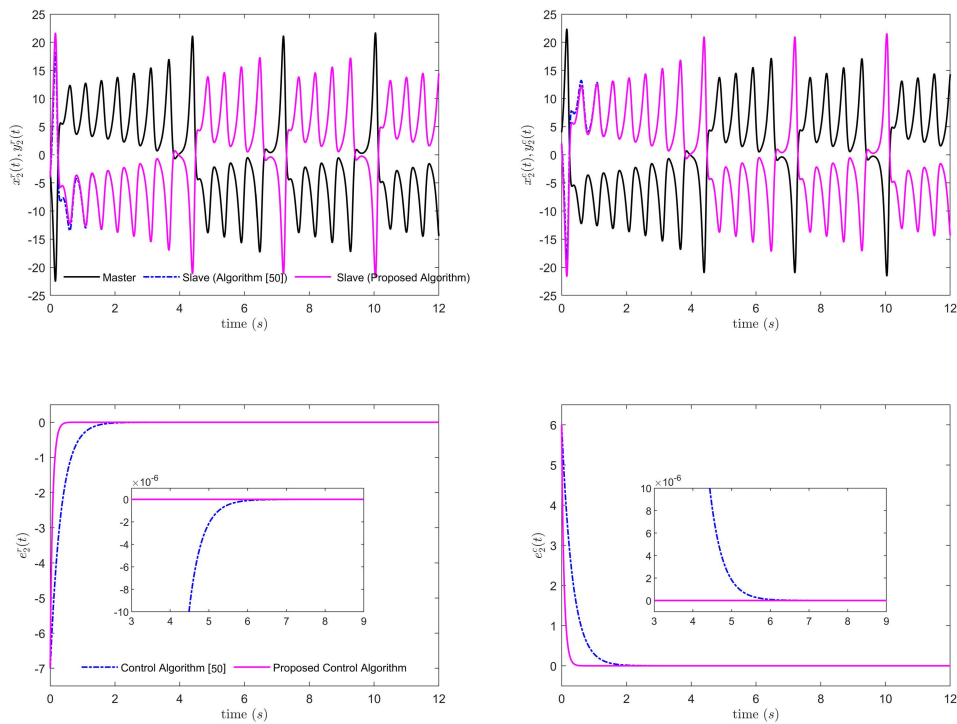
whereas

$$\dot{\mathbf{y}}(t) = \begin{bmatrix} y_1, & y_2, & y_3, & y_4 \end{bmatrix}^T,$$

$$\mathbf{h}(\mathbf{y}(t), \bar{\mathbf{y}}(t), t) = \begin{bmatrix} 14(y_2 - y_1) + jy_4 \\ 40y_1 - y_2 - y_1 y_3 + jy_4 \\ 1/2(\bar{y}_1 y_2 + y_1 \bar{y}_2) - 5y_3 \\ 1/2(\bar{y}_1 y_2 + y_1 \bar{y}_2) - 13y_4 \end{bmatrix},$$

and $\mathbf{u}(t) = \begin{bmatrix} u_1, & u_2, & u_3, & u_4 \end{bmatrix}^T$.

(a) The time histories of the state variables $(x_1^r(t), y_1^r(t), x_1^c(t), y_1^c(t))$ and the CMPS error states $(e_1^r(t), e_1^c(t))$
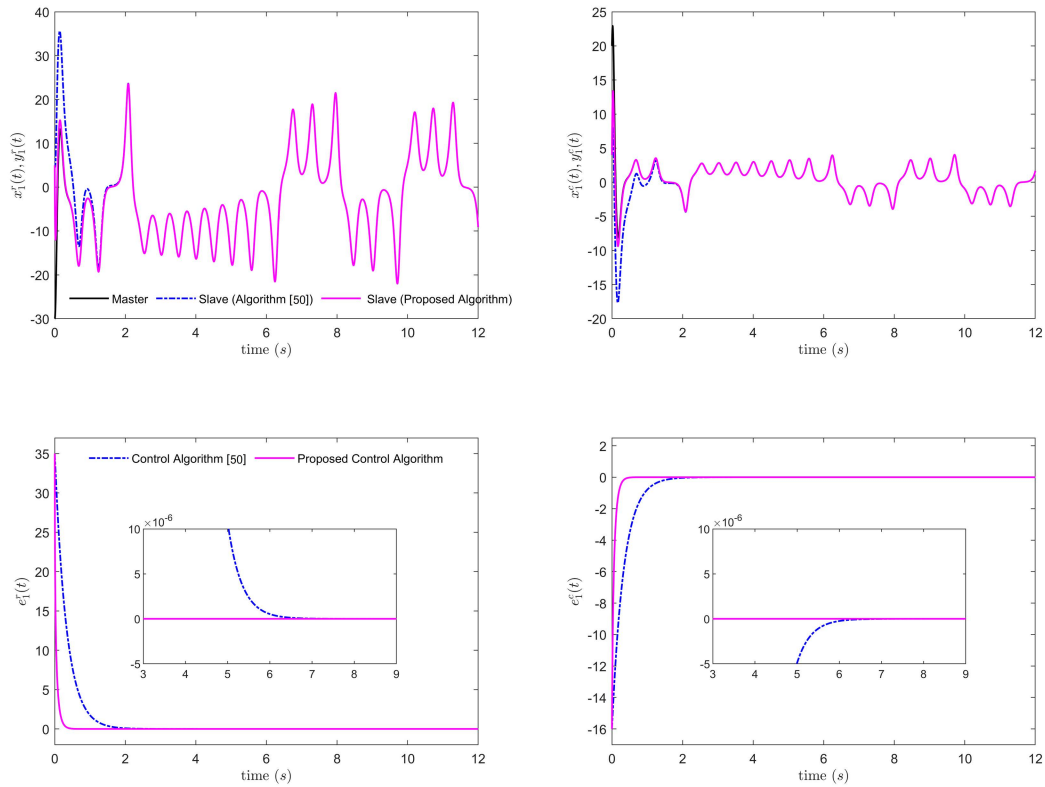

(b) The time histories of the state variables $(x_2^r(t), y_2^r(t), x_2^c(t), y_2^c(t))$ and the CMPS error states $(e_2^r(t), e_2^c(t))$

FIGURE 2. The time histories of the state variables and the CMPS error states between the master system and the slave system under varying time in Case 1.

It is interesting to note that the system (27) and the system (28) have been used for the description or simulation of the physics in the thermal convection of liquid flows or the detuned lasers [51]. The system parameters

used in Eq. (27) and Eq. (28) were exactly cited from the paper [23].

To demonstrate that the upper bound of convergence time does not depend on initial states of the synchronized system,
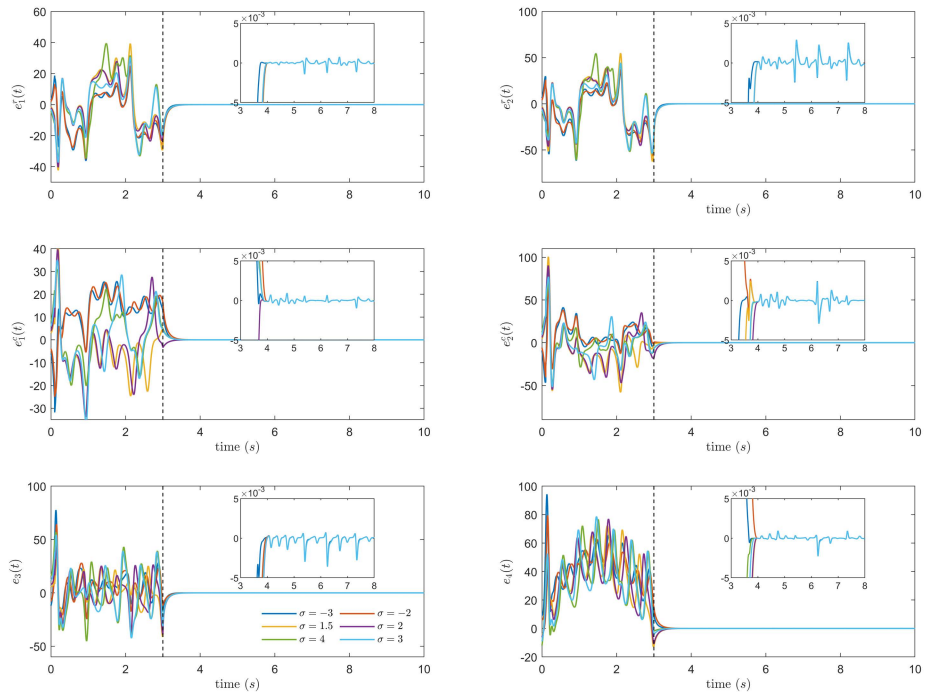
(a) The time histories of the state variables $(x_1^r(t), y_1^r(t), x_1^c(t), y_1^c(t))$ and the CMPS error states $(e_1^r(t), e_1^c(t))$
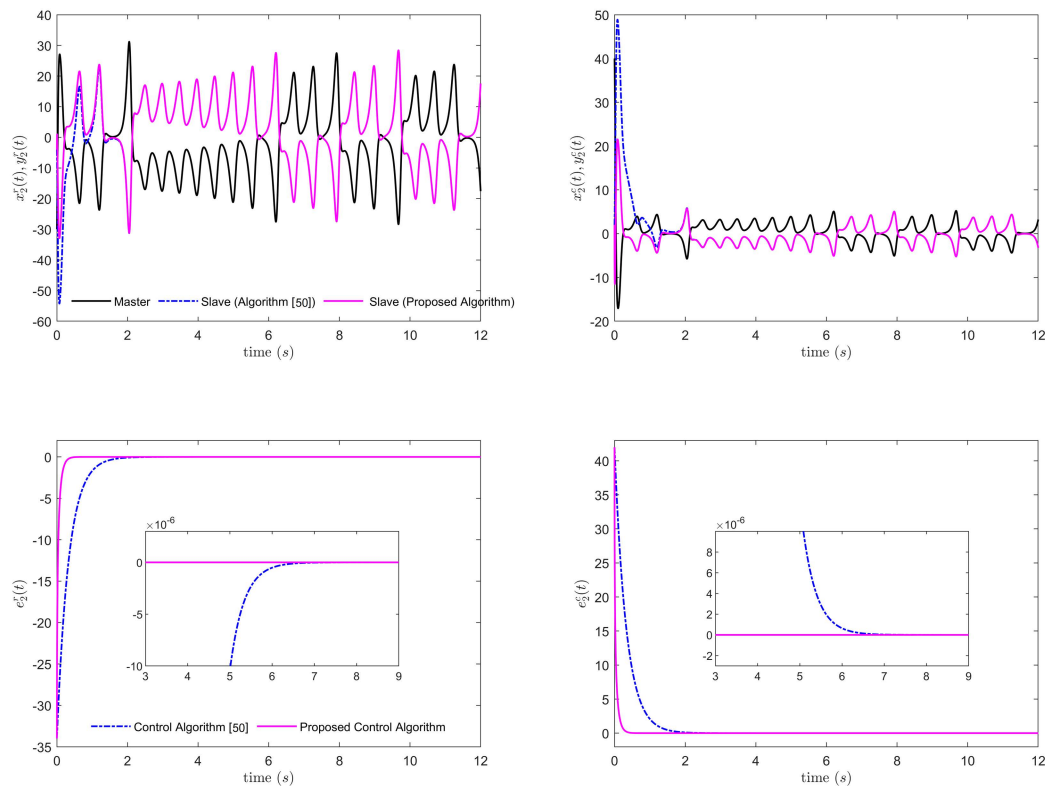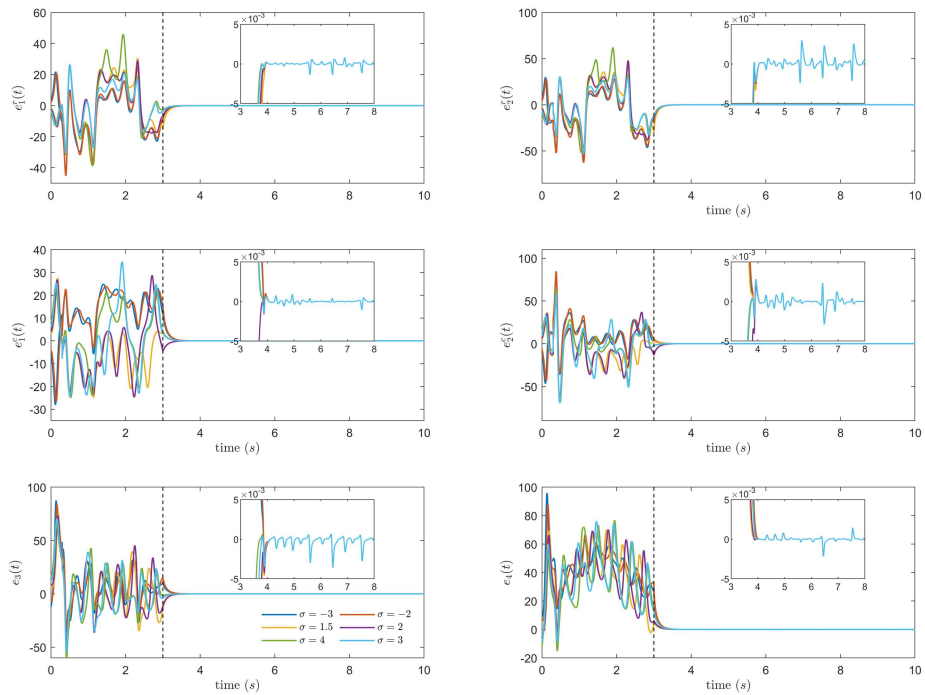

(b) The time histories of state variables $(x_2^r(t), y_2^r(t), x_2^c(t), y_2^c(t))$ and the CMPS error states $(e_2^r(t), e_2^c(t))$

FIGURE 3. The time histories of the state variables and the CMPS error states between the master system and the slave system under varying time in Case 2.

(a) The time histories of the CMFPLS error states in Case: $\tau_1 = 0.1$, $t_0 = 3s$, and $\sigma = \{-3, -2, 1.5, 2, 4, 3\}$

(b) The time histories of the CMFPLS error states in Case: $\tau_2 = 0.3$, $t_0 = 3s$, and $\sigma = \{-3, -2, 1.5, 2, 4, 3\}$

FIGURE 4. The time histories of the CMFPLS error states under varying time.

six different cases have been simulated in the second illustrative example as follows. Six cases correspond to six different values of σ, as reported in Table 5. In addition, all six cases are considered with the two different time delays (τ_1 and τ_2), as shown in Table 5.

The master system (27) and the slave system (28) have the initial conditions $\mathbf{x}(0)$ and $\mathbf{y}(0)$ selected accordingly as in Table 5. To achieve the CMFPLS, the time delay τ and the factor scaling functions ξ are respectively selected according to Table 1 and they are reported in Table 5. The proposed

controller parameters are also assigned as in Table 2 for example 2. From the controller parameter, we can calculate the upper bound of convergence time with $T_2 \approx 1.94s$, which is based on Eq. (24). At a time $t_0 = 3s$, the proposed control inputs are assumed to be impacted to the response system. Therefore, the upper bound of the total convergence time can be calculated as $t_0 + T_2 \approx 4.94s$.

For the second illustrative example, the RMSEs in all cases are calculated at the time when the control signals are activated, as shown in Table 5.

For all cases, the time responses of the CMFPLS errors are exhibited in Fig. 4. The CMFPLS errors reach zero within the period of the fixed-time despite initial conditions. The time convergence of the CMFPLS errors can be obtained within a limited time period that is lesser than $t_0 + T_2 \approx 4.94s$, as shown in Fig. 4. Those initial conditions could be set with arbitrary different values. Obviously, the CMFPLS errors could converge to zero the period of the fixed-time. Consequently, synchronization and stabilization could be achieved within a period of bounded time.

V. CONCLUSION

From the main obtained results in the development of the proposed algorithm, simulation performance results, and comparison with some existing methods, we conclude that the important values of this paper can be summed up as follows: 1) The CMFPLS of HCSs was considered. Applying this system, a new FxTC method was proposed to guarantee synchronization and the desired performance; 2) Synchronization was not only achieved within a predefined limit of time regardless of initial values but also was achieved faster than some existing methods; 3) The settling time has been completely calculated by solving the differential equations and proof of stability and synchronization has been rigorously verified through Lyapunov theory. 4) Two simulation examples were performed in many cases with the change of initial values and time delay of the system to verify the effectiveness of the designed method.

However, it can be seen that the limitation of the paper is that external disturbances have not been considered yet. Therefore, our next work is to research the CMFPLS of HCSs with external disturbances by proposing a new fixed-time SMC to deal with the mentioned systems.

LIST OF ABBREVIATIONS

SMC	Sliding Mode Control
HCSs	Hyperchaotic Complex Systems
AS	Anti-Synchronization
LS	Lag Synchronization
CoS	Complete Synchronization
HCSs	Hyperchaotic Complex Systems
AS	Anti-Synchronization
LAS	Lag Anti-Synchronization
CAS	Complex Anti-Synchronization
CLAS	Complex Lag Anti-Synchronization

LS	Lag Synchronization
CoS	Complete Synchronization
CoLS	Complete Lag Synchronization
PS	Projective Synchronization
PLS	Projective Lag Synchronization
CPLS	Complex Projective Lag Synchronization
FPS	Function Projective Synchronization
FPLS	Function Projective Lag Synchronization
CFPLS	Complex Function Projective Lag Synchronization
MPS	Modified Projective Synchronization
MPLS	Modified Projective Lag Synchronization
MFPS	Modified Function Projective Synchronization
MFPLS	Modified Function Projective Lag Synchronization
CPS	Complex Projective Synchronization
CCoS	Complex Complete Synchronization
CMPS	Complex Modified Projective Synchronization
CMPLS	Complex Modified Projective Lag Synchronization
CFPS	Complex Function Projective Synchronization
CMFPS	Complex Modified Function Projective Synchronization
CMFPLS	Complex Modified Function Projective Lag Synchronization
CCoLS	Complex Complete Lag Synchronization
FnTC	Finite-Time Control
FxTC	Fixed-Time Control
RMSE	Root-Mean-Square Error

APPENDIX

First, we set $q = \vartheta^{\frac{1-\alpha_i}{2}}$, hence,

$$\frac{d\vartheta^{\frac{1-\alpha_i}{2}}}{\left(\kappa_{1i}\vartheta^{1-\alpha_i} + \kappa_{2i}\vartheta^{\frac{1-\alpha_i}{2}} + \kappa_{3i}\right)} = \frac{dq}{\kappa_{1i}\left(q^2 + \frac{\kappa_{2i}}{\kappa_{1i}}q + \frac{\kappa_{3i}}{\kappa_{1i}}\right)}$$

$$= \frac{d\left(q + \frac{\kappa_{2i}}{2\kappa_{1i}}\right)}{\kappa_{1i}\left(\left(q + \frac{\kappa_{2i}}{2\kappa_{1i}}\right) + \left(\frac{4\kappa_{3i}\kappa_{1i} - \kappa_{2i}^2}{4\kappa_{1i}^2}\right)\right)} \quad (29)$$

Then, we set $U = q + \frac{\kappa_{2i}}{2\kappa_{1i}}$ and $a = \frac{\sqrt{4\kappa_{3i}\kappa_{1i} - \kappa_{2i}^2}}{2\kappa_{1i}}$. Therefore,

$$U = a \times \tan v \rightarrow v = \arctan\left(\frac{U}{a}\right)$$

$$\rightarrow dU = a \times \left(\tan^2 v + 1\right) dv \quad (30)$$

$$\frac{dU}{U^2 + a^2} = \frac{a \times \left(\tan^2 v + 1\right) dv}{a^2 \times \tan^2 v + a^2} = \frac{1}{a}dv$$

$$U = \frac{1}{a} \int\limits_{\arctan\left(\frac{U_1}{a}\right)}^{\arctan\left(\frac{U_2}{a}\right)} dv = \frac{1}{a} v \left| \begin{matrix} \arctan\left(\frac{U_2}{a}\right) \\ \arctan\left(\frac{U_1}{a}\right) \end{matrix} \right.$$

$$= \frac{1}{a}\left(\arctan\frac{U_2}{a} - \arctan\frac{U_1}{a}\right) \qquad (31)$$

Eq. (30) is corresponding to

$$= \frac{2}{\sqrt{4\kappa_{3i}\kappa_{1i} - \kappa_{2i}^2}} \begin{pmatrix} \arctan\frac{2\kappa_{1i}}{\sqrt{4\kappa_{3i}\kappa_{1i} - \kappa_{2i}^2}} \\ \times\left(\vartheta^{\frac{1-\alpha_i}{2}}(0) + \frac{\kappa_{2i}}{2\kappa_{1i}}\right) \\ - \arctan\frac{2\kappa_{1i}}{\sqrt{4\kappa_{3i}\kappa_{1i} - \kappa_{2i}^2}} \\ \times\left(\vartheta^{\frac{1-\alpha_i}{2}}(0) + \frac{\kappa_{2i}}{2\kappa_{1i}}\right) \end{pmatrix}$$

$$= \frac{2}{\sqrt{4\kappa_{3i}\kappa_{1i} - \kappa_{2i}^2}} \begin{pmatrix} \arctan\frac{\kappa_{2i}}{\sqrt{4\kappa_{3i}\kappa_{1i} - \kappa_{2i}^2}} \\ - \arctan\frac{2\kappa_{1i}\vartheta^{\frac{1-\alpha_i}{2}}(0) + \kappa_{2i}}{\sqrt{4\kappa_{3i}\kappa_{1i} - \kappa_{2i}^2}} \end{pmatrix} \qquad (32)$$

Consequently,

$$T_\vartheta = \frac{1}{(1-\alpha_i)} \frac{2}{\sqrt{4\kappa_{3i} - \kappa_{2i}^2}}$$

$$\times \left(\arctan\frac{2\kappa_{1i}\vartheta^{\frac{1-\alpha_i}{2}}(0) + \kappa_{2i}}{\sqrt{4\kappa_{3i} - \kappa_{2i}^2}} - \arctan\frac{\kappa_{2i}}{\sqrt{4\kappa_{3i} - \kappa_{2i}^2}}\right) \qquad (33)$$

REFERENCES

[1] M. Bucolo, A. Buscarino, C. Famoso, L. Fortuna, and S. Gagliano, "Imperfections in integrated devices allow the emergence of unexpected strange attractors in electronic circuits," *IEEE Access*, vol. 9, pp. 29573–29583, 2021.

[2] T. Weng, H. Yang, C. Gu, J. Zhang, and M. Small, "Synchronization of chaotic systems and their machine-learning models," *Phys. Rev. E, Stat. Phys. Plasmas Fluids Relat. Interdiscip. Top.*, vol. 99, no. 4, Apr. 2019, Art. no. 42203.

[3] G. M. Mahmoud and T. Bountis, "The dynamics of systems of complex nonlinear oscillators: A review," *Int. J. Bifurcation Chaos*, vol. 14, no. 11, pp. 3821–3846, Nov. 2004.

[4] X. Dai, X. Li, H. Guo, D. Jia, M. Perc, P. Manshour, Z. Wang, and S. Boccaletti, "Discontinuous transitions and rhythmic states in the D-dimensional Kuramoto model induced by a positive feedback with the global order parameter," *Phys. Rev. Lett.*, vol. 125, no. 19, Nov. 2020, Art. no. 194101.

[5] X. Dai, X. Li, R. Gutiérrez, H. Guo, D. Jia, M. Perc, P. Manshour, Z. Wang, and S. Boccaletti, "Explosive synchronization in populations of cooperative and competitive oscillators," *Chaos, Solitons Fractals*, vol. 132, Mar. 2020, Art. no. 109589.

[6] B. Sun, M. Li, F. Zhang, H. Wang, and J. Liu, "The characteristics and self-time-delay synchronization of two-time-delay complex Lorenz system," *J. Franklin Inst.*, vol. 356, no. 1, pp. 334–350, Jan. 2019.

[7] A. C. Fowler, J. D. Gibbon, and M. J. McGuinness, "The real and complex Lorenz equations and their relevance to physical systems," *Phys. D, Nonlinear Phenomena*, vol. 7, nos. 1–3, pp. 126–134, May 1983.

[8] X. Wu, C. J. Zhu, and H. B. Kan, "An improved secure communication scheme based passive synchronization of hyperchaotic complex nonlinear system," *Appl. Math. Comput.*, vol. 252, pp. 201–214, Feb. 2015.

[9] C. Huang and J. Cao, "Active control strategy for synchronization and anti-synchronization of a fractional chaotic financial system," *Phys. A, Stat. Mech. Appl.*, vol. 473, pp. 262–275, May 2017.

[10] F. Zhang, "Lag synchronization of complex Lorenz system with applications to communication," *Entropy*, vol. 17, no. 12, pp. 4974–4985, Jul. 2015.

[11] E. M. Shahverdiev, S. Sivaprakasam, and K. A. Shore, "Lag synchronization in time-delayed systems," *Phys. Lett. A*, vol. 292, no. 6, pp. 320–324, Jan. 2002.

[12] I. A. Korneev, V. V. Semenov, A. V. Slepnev, and T. E. Vadivasova, "Complete synchronization of chaos in systems with nonlinear inertial coupling," *Chaos, Solitons Fractals*, vol. 142, Jan. 2021, Art. no. 110459.

[13] T. Banerjee, D. Biswas, and B. C. Sarkar, "Anticipatory, complete and lag synchronization of chaos and hyperchaos in a nonlinear delay-coupled time-delayed system," *Nonlinear Dyn.*, vol. 72, pp. 321–332, Apr. 2013.

[14] R. Guo, "Projective synchronization of a class of chaotic systems by dynamic feedback control method," *Nonlinear Dyn.*, vol. 90, no. 1, pp. 53–64, Oct. 2017.

[15] J. Liu, S. Liu, and C. Yuan, "Adaptive complex modified projective synchronization of complex chaotic (hyperchaotic) systems with uncertain complex parameters," *Nonlinear Dyn.*, vol. 79, no. 2, pp. 1035–1047, 2015.

[16] G. M. Mahmoud and E. E. Mahmoud, "Modified projective lag synchronization of two nonidentical hyperchaotic complex nonlinear systems," *Int. J. Bifurcation Chaos*, vol. 21, no. 8, pp. 2369–2379, Aug. 2011.

[17] J. Fang, N. Liu, and J. Sun, "Adaptive modified function projective synchronization of uncertain complex dynamical networks with multiple time-delay couplings and disturbances," *Math. Problems Eng.*, vol. 2018, pp. 1–11, 2018.

[18] F. Nian, X. Liu, Y. Zhang, and X. Yu, "Module-phase synchronization of fractional-order complex chaotic systems based on RBF neural network and sliding mode control," *Int. J. Modern Phys. B*, vol. 34, no. 7, Mar. 2020, Art. no. 2050050.

[19] Q. Xu, X. Xu, S. Zhuang, J. Xiao, C. Song, and C. Che, "New complex projective synchronization strategies for drive-response networks with fractional complex-variable dynamics," *Appl. Math. Comput.*, vol. 338, pp. 552–566, Dec. 2018.

[20] G. M. Mahmoud, E. E. Mahmoud, and A. A. Arafa, "Synchronization of time delay systems with non-diagonal complex scaling functions," *Chaos, Solitons Fractals*, vol. 111, pp. 86–95, Jun. 2018.

[21] F.-F. Zhang, S.-T. Liu, and W.-Y. Yu, "Modified projective synchronization with complex scaling factors of uncertain real chaos and complex chaos," *Chin. Phys. B*, vol. 22, no. 12, Dec. 2013, Art. no. 120505.

[22] F. Nian, X. Wang, Y. Niu, and D. Lin, "Module-phase synchronization in complex dynamic system," *Appl. Math. Comput.*, vol. 217, no. 6, pp. 2481–2489, Nov. 2010.

[23] E. E. Mahmoud, "Complex complete synchronization of two nonidentical hyperchaotic complex nonlinear systems," *Math. Methods Appl. Sci.*, vol. 37, no. 3, pp. 321–328, Feb. 2014.

[24] C.-M. Jiang, S.-T. Liu, and F.-F. Zhang, "Complex modified projective synchronization for fractional-order chaotic complex systems," *Int. J. Autom. Comput.*, vol. 15, no. 5, pp. 603–615, Oct. 2018.

[25] S. Liu and F. Zhang, "Complex function projective synchronization of complex chaotic system and its applications in secure communication," *Nonlinear Dyn.*, vol. 76, no. 2, pp. 1087–1097, 2014.

[26] J. Liu and S. Liu, "Complex modified function projective synchronization of complex chaotic systems with known and unknown complex parameters," *Appl. Math. Model.*, vol. 48, pp. 440–450, Aug. 2017.

[27] C. Zhang, X. Wang, X. Ye, S. Zhou, and L. Feng, "Robust modified function projective lag synchronization between two nonlinear complex networks with different-dimensional nodes and disturbances," *ISA Trans.*, vol. 101, pp. 42–49, Jun. 2020.

[28] S. Karimi, S. Effati, and F. H. Ghane, "The synchronization of chaotic systems applying the parallel synchronization method," *Phys. Scripta*, vol. 94, no. 10, Oct. 2019, Art. no. 105215.

[29] B. Quan, C. Wang, J. Sun, and Y. Zhao, "A novel adaptive active control projective synchronization of chaotic systems," *J. Comput. Nonlinear Dyn.*, vol. 13, no. 5, pp. 1–10, May 2018.

[30] H. Takhi, K. Kemih, L. Moysis, and C. Volos, "Passivity based control and synchronization of perturbed uncertain chaotic systems and their microcontroller implementation," *Int. J. Dyn. Control*, vol. 8, pp. 973–990, Mar. 2020.

[31] A. Sambas, M. Mamat, A. A. Arafa, G. M. Mahmoud, M. A. Mohamed, and W. S. M. Sanjaya, "A new chaotic system with line of equilibria: Dynamics, passive control and circuit design," *Int. J. Electr. Comput. Eng.*, vol. 9, no. 4, p. 2336, Aug. 2019.

[32] B. Vaseghi, S. Mobayen, S. S. Hashemi, and A. Fekih, "Fast reaching finite time synchronization approach for chaotic systems with application in medical image encryption," *IEEE Access*, vol. 9, pp. 25911–25925, 2021.

[33] D. Zhang, J. Mei, and P. Miao, "Global finite-time synchronization of different dimensional chaotic systems," *Appl. Math. Model.*, vol. 48, pp. 303–315, Aug. 2017.

[34] X.-T. Tran and H.-J. Kang, "Continuous adaptive finite-time modified function projective lag synchronization of uncertain hyperchaotic systems," *Trans. Inst. Meas. Control*, vol. 40, no. 3, pp. 853–860, Feb. 2018.

[35] A. T. Vo, T. N. Truong, and H.-J. Kang, "A novel tracking control algorithm with finite-time disturbance observer for a class of second-order nonlinear systems and its applications," *IEEE Access*, vol. 9, pp. 31373–31389, 2021.

[36] X. Guo, G. Wen, Z. Peng, and Y. Zhang, "Global fixed-time synchronization of chaotic systems with different dimensions," *J. Franklin Inst.*, vol. 357, no. 2, pp. 1155–1173, Jan. 2020.

[37] M. Shirkavand and M. Pourgholi, "Robust fixed-time synchronization of fractional order chaotic using free chattering nonsingular adaptive fractional sliding mode controller design," *Chaos, Solitons Fractals*, vol. 113, pp. 135–147, Aug. 2018.

[38] A. T. Vo, T. N. Truong, and H.-J. Kang, "A novel fixed-time control algorithm for trajectory tracking control of uncertain magnetic levitation systems," *IEEE Access*, vol. 9, pp. 47698–47712, 2021.

[39] X.-T. Tran and H.-J. Kang, "Fixed-time complex modified function projective lag synchronization of chaotic (Hyperchaotic) complex systems," *Complexity*, vol. 2017, pp. 1–9, Jan. 2017.

[40] S. Yu, X. Yu, and R. J. Stonier, "Continuous finite-time control for robotic manipulators with terminal sliding mode," *Automatica*, vol. 41, no. 11, pp. 1957–1964, 2005.

[41] E. M. Fels, "Beckenbach," in *Inequalities*, R. Bellman, Ed. Berlin, Germany: Springer-Verlag, 1961.

[42] Q. Li and C. Yue, "Predefined-time modified function projective synchronization for multiscroll chaotic systems via sliding mode control technology," *Complexity*, vol. 2020, pp. 1–11, Aug. 2020.

[43] H. K. Khalil, "Chapter 13: State feedback stabilization," in *Nonlinear Systems*, 3rd, ed. Upper Saddle River, NJ, USA: Prentice-Hall, 2002, pp. 197–227.

[44] A. Buscarino, L. Fortuna, and L. Patanè, "Master-slave synchronization of hyperchaotic systems through a linear dynamic coupling," *Phys. Rev. E, Stat. Phys. Plasmas Fluids Relat. Interdiscip. Top.*, vol. 100, no. 3, Sep. 2019, Art. no. 032215.

[45] P. Arena, A. Buscarino, L. Fortuna, and L. Patanè, "Lyapunov approach to synchronization of chaotic systems with vanishing nonlinear perturbations: From static to dynamic couplings," *Phys. Rev. E, Stat. Phys. Plasmas Fluids Relat. Interdiscip. Top.*, vol. 102, no. 1, Jul. 2020, Art. no. 012211.

[46] S. Junwei, W. Yan, W. Yanfeng, and S. Yi, "Finite-time synchronization between two complex-variable chaotic systems with unknown parameters via nonsingular terminal sliding mode control," *Nonlinear Dyn.*, vol. 85, no. 2, pp. 1105–1117, 2016.

[47] J. Sun, G. Cui, Y. Wang, and Y. Shen, "Combination complex synchronization of three chaotic complex systems," *Nonlinear Dyn.*, vol. 79, no. 2, pp. 953–965, Jan. 2015.

[48] J. Sun, S. Yi, X. Wang, and C. Jie, "Finite-time combination-combination synchronization of four different chaotic systems with unknown parameters via sliding mode control," *Nonlinear Dyn.*, vol. 76, no. 1, pp. 383–397, 2014.

[49] J. Sun, Y. Shen, Q. Yin, and C. Xu, "Compound synchronization of four memristor chaotic oscillator systems and secure communication," *Chaos, Interdiscipl. J. Nonlinear Sci.*, vol. 23, no. 1, Mar. 2013, Art. no. 013140.

[50] G. M. Mahmoud and E. E. Mahmoud, "Complex modified projective synchronization of two chaotic complex nonlinear systems," *Nonlinear Dyn.*, vol. 73, pp. 2231–2240, Sep. 2013.

[51] E. M. Mahmoud and G. M. Mahmoud, *Chaotic and Hyperchaotic Nonlinear Systems*. Germany: Lambert Academic Publishing, 2011.

ANH TUAN VO received the Bachelor of Science (diploma) degree in electrical engineering from the University of Science and Technology, in 2008, the Master of Science (diploma) degree in automation from The University of Da Nang, Da Nang, Vietnam, in 2013, and the Doctor of Philosophy (diploma) degree in electrical engineering from the Graduate School, University of Ulsan, Ulsan, South Korea, in 2021. He has published more than 25 papers in journals and international conferences. His research interests include intelligent control, sliding mode control and its applications, and fault-tolerant control.

THANH NGUYEN TRUONG received the Bachelor of Science (diploma) degree in electrical engineering from the University of Science and Technology, Da Nang, Vietnam, in 2018. He is currently pursuing the Doctor of Philosophy degree in electrical engineering with the University of Ulsan, Ulsan, South Korea. His research interests include robotic manipulators, sliding mode control and its applications, and advanced control theory for mechatronics.

HEE-JUN KANG received the Bachelor of Science degree in mechanical engineering from Seoul National University, South Korea, in 1985, and the Master of Science and Doctor of Philosophy degrees in mechanical engineering from The University of Texas at Austin, USA, in 1988 and 1991, respectively. He joined the University of Ulsan, in 1992, where he is currently a Professor of electrical engineering. In addition to sensor-based robotics, haptics, robot fault diagnosis, and mechanisms analysis, his current research interests include encompass robot calibration, robot calibration, haptics, and mechanism analysis.

● ● ●